SANDIA REPORT

SAND2015-0538
Unlimited Release
Printed January 2015

Experiments to Populate and Validate a Processing Model for Polyurethane Foam: Additional Data for Structural Foams

Lisa Mondy, Casper Brady, Melissa Soehnel, Christine Roberts, Bion Shelden, Rekha Rao, Mat Celina, Nicholas Giron, Kevin Long, Edward Russick

Prepared by
Sandia National Laboratories
Albuquerque, New Mexico 87185 and Livermore, California 94550

Sandia National Laboratories is a multi-program laboratory managed and operated by Sandia Corporation, a wholly owned subsidiary of Lockheed Martin Corporation, for the U.S. Department of Energy's National Nuclear Security Administration under contract DE-AC04-94AL85000.

Issued by Sandia National Laboratories, operated for the United States Department of Energy by Sandia Corporation.

Available to DOE and DOE contractors from
U.S. Department of Energy
Office of Scientific and Technical Information
P.O. Box 62
Oak Ridge, TN 37831

Telephone: (865) 576-8401
Facsimile: (865) 576-5728
E-Mail: reports@adonis.osti.gov
Online ordering: http://www.osti.gov/bridge

Available to the public from
U.S. Department of Commerce
National Technical Information Service
5285 Port Royal Rd.
Springfield, VA 22161

Telephone: (800) 553-6847
Facsimile: (703) 605-6900
E-Mail: orders@ntis.fedworld.gov
Online order: http://www.ntis.gov/help/ordermethods.asp?loc=7-4-0#online

SAND2015-0538
Unlimited Release
Printed September 2014

Experiments to Populate and Validate a Processing Model for Polyurethane Foam: Additional Data for Structural Foams

Lisa Mondy, Casper Brady, Melissa Soehnel, Christine Roberts, Bion Shelden
Thermal and Fluid Experimental Sciences

Rekha Rao
Fluid Sciences & Engineering

Mat Celina, Nicholas Giron,
Materials Characterization and Performance

Kevin Long
Solid Mechanics

Edward Russick
Packaging & Polymer Processing

Sandia National Laboratories
P.O. Box 5800
Albuquerque, New Mexico 87185-MS0346

Abstract

We are developing computational models to help understand manufacturing processes, final properties and aging of structural foam, polyurethane PMDI. The resulting model predictions of density and cure gradients from the manufacturing process will be used as input to foam heat transfer and mechanical models. BKC 44306 PMDI-10 and BKC 44307 PMDI-18 are the most prevalent foams used in structural parts. Experiments needed to parameterize models of the reaction kinetics and the equations of motion during the foam blowing stages were described for BKC 44306 PMDI-10 in the first of this report series (Mondy et al. 2014). BKC 44307 PMDI-18 is a new foam that will be used to make relatively dense structural supports via over packing. It uses a different catalyst than those in the BKC 44306 family of foams; hence, we expect that the reaction kinetics models must be modified. Here we detail the experiments needed to characterize the reaction kinetics of BKC 44307 PMDI-18 and suggest parameters for the model based on these experiments. In addition, the second part of this report describes data taken to provide input to the preliminary nonlinear viscoelastic structural response model developed for BKC 44306 PMDI-10 foam. We show that the standard cure schedule used by KCP does not fully cure the material, and, upon temperature elevation above 150^{o}C, oxidation or decomposition reactions occur that alter the composition of the foam. These findings suggest that achieving a fully cured foam part with this formulation may be not be possible through thermal curing. As such, viscoelastic characterization procedures developed for curing thermosets can provide only approximate material properties, since the state of the material continuously evolves during tests.

Acknowledgments

The authors would like to acknowledge helpful discussions with Heather Boldt (2153), Christine Mitchell and Joe Fonseca (2128), and personnel at National Nuclear Security Administration's Kansas City Plant, Operated by Honeywell Federal Manufacturing & Technologies, LLC, including James Mahoney, James Tinsley, Audrey Chase, Michael Batrick, and Vinita Chhahira. Also much appreciated are the informative discussions regarding the design of the structural response models with Jamie Kropka, Nick Wyatt, Mark Stavig (1835) and Bob Chambers (1526).

CONTENTS

FIGURES

TABLES

INTRODUCTION

Polyurethane foams are used frequently to mitigate shock and vibration and offer a good compromise between strength and weight. Polyurethanes are chemically blown foams that begin as two-part mixtures, with polyisocyanate in one (T-component) and polyol, water, surfactant and catalyst in the other (R-component). When mixed together, several competing reactions occur simultaneously, the most important of which are the polymerization reaction and the foaming reaction. The major polymerization reaction is that of isocyanate and polyol to form crosslinked polyurethane. Gas is formed when isocyanate reacts with water to produce carbamic acid, which then decomposes to generate CO_2 and an amine group [Tesser 2004]. The relative rates of the foaming and curing reactions dictate the pot life (time during which the material can be poured or injected into a mold), as well as the height the foam can obtain in a specific mold before vitrification halts the volume expansion. The reactions are exothermic and, as foam is a good insulator, can cause the foam itself to char if the part thickness is sufficient.

A production-level foam-processing computational model has been developed through a partnership among WSEAT, ASC, and Systems. The current model is being used to troubleshoot encapsulation process designs and to reduce voids and density gradients and highlight possible areas of higher temperature due to the reaction exotherm. Collecting data on this complex system, with chemical reactions inducing phase changes (both liquid to gas and liquid to solid), heterogeneous microstructure of the foam, and temperature changes from the exothermic reactions, is challenging. To simply measure changes as a function of time and temperature to create purely empirical models would not allow the flexibility and accuracy needed in a process model to predict the manufacture of a wide variety of foamed parts. The current models, based on the physics as we know them, are difficult to parameterize, but it is hoped that, as more experiments are completed, the engineering process model will continue to be developed and refined. The kinetic model described here only applies to the foam during the expansion phase. Further refinement in the kinetic model will be needed to predict the development of cure stresses after the foam expansion has stopped; and this will not be addressed here except cursorily.

As the models mature, we plan to use them to support mold design for structural parts. Because extent-of-cure, density gradients, and residual stresses can exist in the part after it is taken from the mold, dimensional stability of the material as it ages will depend on the manufacturing process as well as post manufacturing environmental exposure. Hence, we expect that the foam process model will be needed as the first part of a cradle-to-grave modeling capability. To this end, we have begun to develop appropriate models for structural foams in addition to encapsulation foams.

The equations and the experimental methods used to populate the parameters in the current processing model are described in Mondy et al 2014. More theory and details of the numerical methods use are described in other publications [Mondy et al. 2010, Rao et al. 2010, 2013]. In Part I of this report we will only briefly describe the experiments used to obtain the appropriate kinetic model parameters for the newly developed, relatively dense, structural foam, BKC 44307 PMDI-18. This structural foam is based on formulations originally developed for encapsulation foams, with a slower acting catalyst than used in another structural foam family BKC 44306.

PMDI-18 has a nominal free rise density of 18 lb/ft^3, hence the addition of that number at the end of the name. A much less dense foam PMDI-4 has been characterized for our models previously [Mondy et al. 2010, Rao et al. 2010, 2013]. The model includes mixture theory formulations for thermal properties, as well as rheology, based on gas fraction. Because these are not expected to be significantly different than the PMDI-4, corrected appropriately for the difference in gas fraction, these tests were not repeated for the PMDI-18. However, there has been evidence that the foaming and curing reactions are not completely independent, but have interactions that affect the reaction rates [Mondy et al. 2010]. Thus, it was desirable to determine the reaction kinetics of this foam and compare the parameters to that of the lighter foam.

Part II of this report describes the data obtained to help begin the development of a structural response model [Long et al. 2014]. The motivation to develop this model comes from the observation that foams have been shown to have dimensional instability, and possible warpage, as they age, which is dependent on the manufacturing history [Pockett and Warriner, 2013]. During the foaming process, the material expands to fill the mold until the polymer matrix gels. Post gelation, the polymer matrix is a curing, viscoelastic solid, and it is likely that additional water-isocyanate reactions produce gas that over-pressurizes existing pores within the polymer matrix without increasing foam volume. Continued curing causes the polymer matrix to shrink in volume, but because the foam is constrained by the surrounding mold, residual stresses arise. Continued cure also causes the equilibrium shear modulus of the matrix phase, as well as that of the macroscale foam, to increase, which heightens the residual stress state. The glass transition temperature (T_g) of the matrix phase also increases with extent of cure. These processes continue until the evolving T_g approaches the local temperature in the curing foam after which, the sluggish viscoelastic time scale arrests the reaction kinetics. Following the oven cure, the foam part is cooled to room temperature out of the mold and may shrink primarily due to the coefficient of thermal expansion (CTE) of the material. When the material is released from the mold, residual manufacturing stresses can cause the foamed component to change shape. Following significant efforts from Sandia scientists over the course of twenty years or more [see for example Adolf, Chambers, and Neidigk 2009; Adolf and Chambers 2007], Long *et al.* adapted a formulation for curing solid polymer systems to this scenario of a curing foam with spatial variations in extent of cure and density.

The base case structural response model will be developed for BKC 44306 PMDI-10 foam. Coefficient of thermal expansion (CTE) was measured with thermo-mechanical analysis (TMA) on several samples of this foam, both for a sample real part (Support A) manufactured according to the Kansas City Plant (KCP) protocol and for a sample made in a similar manner but from the foam precursors with as much water removed as practical to produce a cured polymer with very little porosity (what we will call the cured polymer matrix). In addition to the CTE these tests give an approximate value for the glass transition temperature (T_g) of the final foam part.

In addition, rheological experiments were performed to help define the parameters of the viscoelastic model. The model, as originally envisioned, required parameters defined from a fully cured material. As will be shown, the standard KCP protocol does not result in a fully cured material, and in fact removing all of the unreacted isocyanate causes additional, as yet undefined reactions and material embrittlement (accelerated aging). These experiments of discovery have shown that the viscoelastic modeling must be approached differently.

PART I. PMDI-18 REACTION KINETICS

I.2. Foam Material

The recipes for the BKC 44307 PMDI-18 foam components R and T are shown in Table 1, in parts by weight. Unlike the BKC 44306 family of foams, this foam includes some prepolymer in the T component (a small amount of polyol is mixed with the isocyanate and hence reacts). The R to T mix ratio is 40.3 to 59.7 parts by weight [Russick, 2014], resulting in the overall mass fraction of components before any reaction occurs that is also shown in the table. This mixture results in NCO functional groups (cyanates) being 15-20% in excess of a stoichiometric ratio.

Table 1. BKC 44307 PMDI-18 Structural Foam Formulation

Material	***Specification***	***PBW***
R-Component		
Voranol 490 (polyol)	2170369	100
Water		0.3
Dabco DC-197 (surfactant)	6500617	2.0
33LV (catalyst)	2170328	0.15
T-Component		
PAPI 27 (isocyanate)	4612092	100
Voranol 490 (polyol)	2170369	2.6

Overall initial formula	***Mass fraction***
polyol	0.40849
water	0.00118
surfactant	0.00787
catalyst	0.00059
isocyanate	0.58187

I.3. Result of Experiments to Obtain Model Input Data

I.3.1. Polymerization

Micro-attenuated total reflection (ATR) infrared spectroscopy (IR) measurements, taken with a Bruker Equinox 55 spectrometer with a deuterated triglycine sulfate (DTGS) detector (ID301/8) operating at room temperature, were used to establish the cure conversion kinetics and determine

the activation energy as described previously [Rao et al. 2010, Mondy et al. 2014]. The peak at 1218 cm^{-1} represents the pure curing reaction, as it relates to the C=O-O-R linkage (i.e., the ester side of the urethane) between the polyol and urethane group. Successive IR spectra were acquired over time, and the relative absorbance changes for specific bands provided time dependent cure-state information.

The height of the 1218 cm^{-1} band as it evolves in time for experiments at several constant temperatures is plotted in Figure 1.

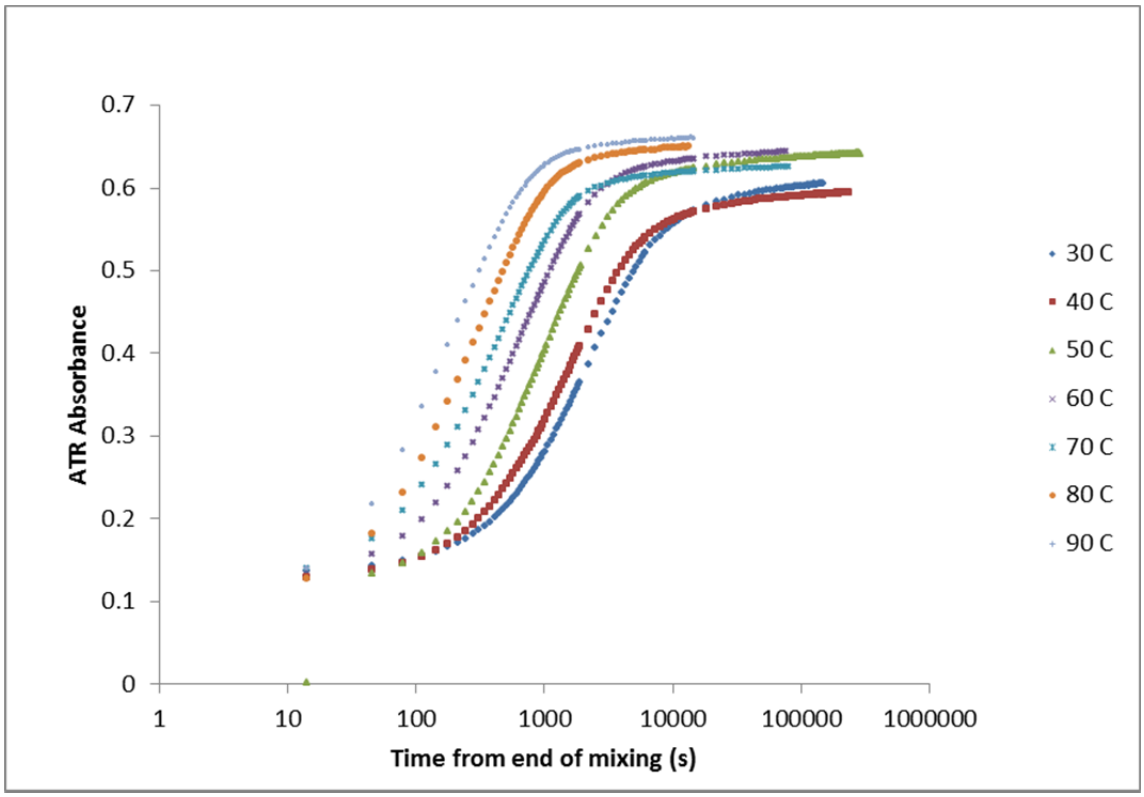

Figure 1. Plot of data for the 1218 cm^{-1} peak height for PMDI-18 foam.

I.3.2. Foam Rise in a Channel

Unfortunately, no specific peak in the IR spectrum exists for the foaming reaction, first of all since the carbamic acid generating CO_2 is a transient species, and secondly since after decomposition the resulting urea linkages (carbonyl and amide groups) overlap with the urethanes in the spectrum. Therefore, a different method must be used to determine the foaming reaction rates.

In order to estimate the rate of gas formation, we observe the height evolution of a foam column with time and assume that the increase in volume is solely due to the production of CO_2. This method is somewhat inadequate as it cannot account for all the CO_2 produced as some is lost to the atmosphere through the free surface and does not produce an increase in volume, and some remains supersaturated in solution and does not nucleate to form gas bubbles. Because the reaction is exothermic and because the foam precursor materials cannot be preheated to high

temperatures or the water will evaporate and not be available for the foaming reaction, these height-vs.-time experiments cannot be done under isothermal conditions, unlike the IR spectrophotometry. As mentioned in Mondy et al. [2010], there is some evidence that the foaming reaction is influenced by the polymerization reaction; therefore, we did not attempt to measure the foaming reaction rate in a model system, but instead settled on measuring the foaming reaction in the real system

Past data has shown that the blowing reaction can produce pressurized bubbles, especially after the continuous phase becomes viscous and slows the foam rise [Mondy et al. 2014]. Therefore, not only volume change, but also temperature and pressure are measured. Temperature is measured at three locations along the centerline of the mold and pressure is measured at the back wall, as shown in Figure 2. The number of moles of CO_2, $n_{CO2,}$ is then estimated through the ideal gas law ($n_{CO2}=PV/RT$, where V is volume, P is the pressure, R is the universal gas constant, and T is the temperature). By doing this, we are assuming that the pressure at the wall is representative of the pressure in the bubbles and that volume change due to temperature of the liquid phase is negligible, as is any volume change from the depletion of the small amount of H_2O in the system and reactions not producing gas.

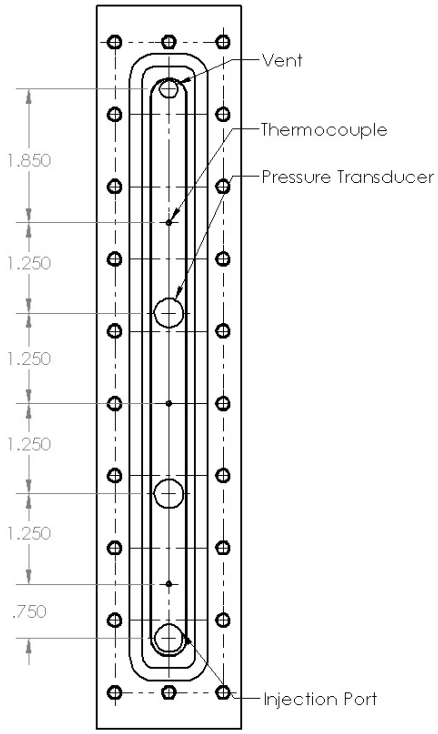

Figure 2. Sketch of channel mold used to measure the evolution of gas during foaming. Dimensions are in inches.

Experiments were repeated at four nominal oven temperatures, 40, 50, 60, and 70°C, with the method described previously. Examples of typical raw data, details on error estimation, and more

in-depth description of the analysis method can be found in Mondy et al. [2014]. Briefly, an extent of reaction as a function of time was calculated for each experiment, where the extent of reaction was the calculated number of moles based on the ideal gas law divided by the maximum number from stoichiometry. Every mole of H_2O produces one mole of CO_2; therefore, the maximum number of moles of CO_2 can be calculated from the mass fraction of H_2O listed in Table 1 multiplied by the mass injected and then converted to moles by dividing by the molecular weight of H_2O. The resulting extent-of reactions with time are shown in Figure 3, where the black curves are uncertainty bars on the experimental results. The parameters to produce the model curve fits will be discussed in the next section.

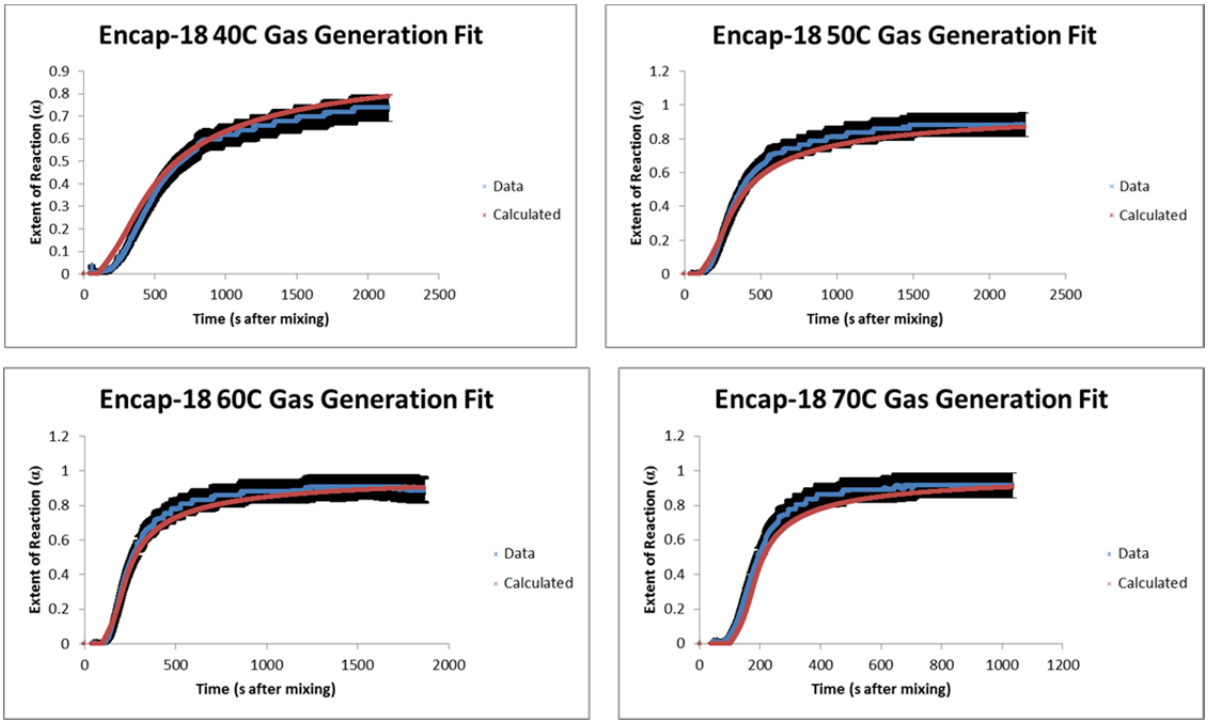

Figure 3. Extent of gas generation reaction data (blue line) for BKC 44307 PMDI-18 foam at nominal oven temperatures listed in each title. Black bands indicate 8% uncertainty bars. Red curves are the model results with parameters listed in the text.

I.4. Model Parameter Determination

I.4.1. Polymerization

As before [Mondy et al. 2014], we say that the polymerization reaction kinetics follows condensation chemistry and that the reaction rate can be written as [May 1988; Adolf 1996]:

$$\frac{d\xi}{dt} = k(1-\xi)^q(A+\xi^p) \tag{1}$$

$$k = k_0 e^{E_\xi / RT} \tag{2}$$

where ξ is the extent of the polymerization reaction, k_o is the rate coefficient, E_ξ is the activation energy, R is the universal gas constant, A is a constant, and q and p are the orders of reaction.

Note that it is likely that the material is vitrifying during the experiment, and the form of the reaction rate as written above will not capture the diffusion limited regime occuring at later times. Because, for now we are only interested in the early time reaction rates (to predict the behavior during the foam rise), this will not be addressed. Implications will be discussed more in the following paragraphs and in the conclusion.

The kinetic cure curves (Figure 1) were normalized by the lowest and highest peak height seen across the range of temperatures so that the values ranged between 0 and 1, thus giving an estimate of the extent of reaction. It is interesting to note that the maximum peak height is not a clear function of T, as would be expected if the material were vitrifying during the test (one would expect that the reaction would progress further with increasing temperature). At this time, we will simply normalize with the peak height corresponding to the case where the reaction has progressed the furthest of all cases. The curves were then time-temperature shifted (Figure 4). Time shifting to a single reference temperature is performed by multiplying the time at any temperature T by a shift factor a_T that causes the data to approximately overlay during the time of most interest (during foaming, less than 1000s). These shift factors, or relative reactivity ratios, can then be used to determine E_ξ for the Arrhenius rate constant. A plot of the natural logarithm of the shift factors versus the inverse of temperature in Kelvin yields a linear plot, the slope of which gives E_ξ. Figure 5 shows the resulting Arrhenius plot for the PMDI-18 foam data.

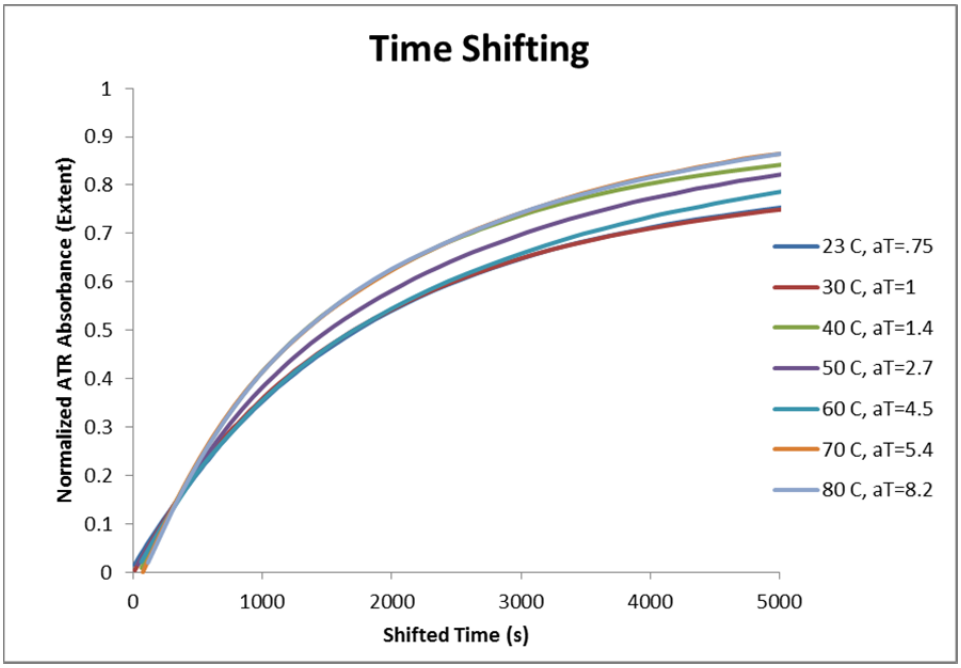

Figure 4. Shifted plot for PMDI-18 foam, with shift factors noted.

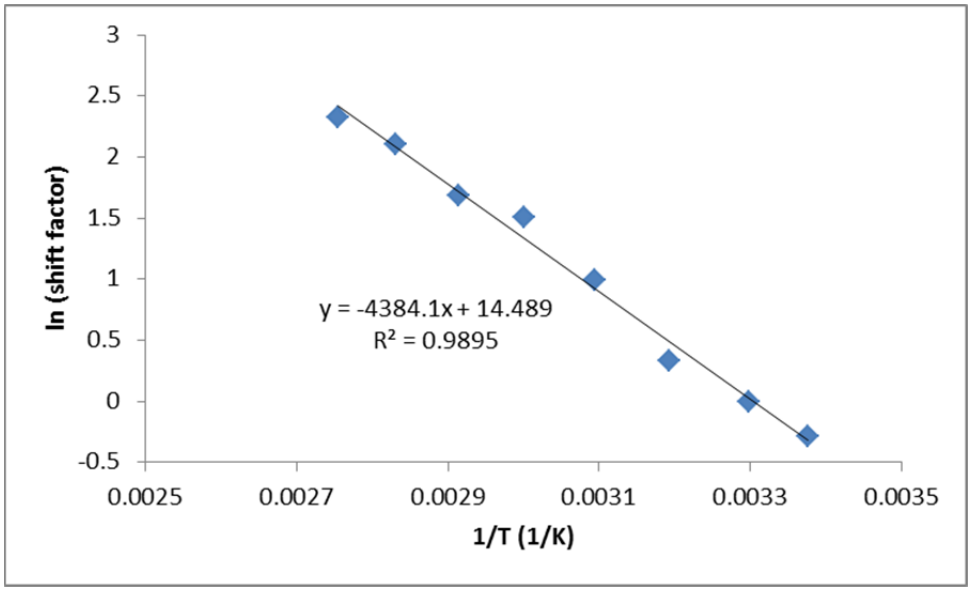

Figure 5.Activation energy (E_ξ/R) given from the time shift factors. Here, E_ξ/R=4384.1 K.

The reaction coefficient k was estimated from the initial reaction rates at 30°C, to be consistent with the fitting protocol done for the PMDI-10 structural foam [Mondy et al. 2014]. This value is about 0.005 s^{-1}.

A rough value of k=0.005 s^{-1} at 30°C, combined with the Arrhenius fit from Figure 5, yields a value for k_0 of 954.2 s^{-1}. The remaining parameters in equations 1 and 2, p, q, A, were varied until the equation best described the IR data during the foam expansion phase (the first several thousand seconds). The best fit of the data was achieved with the following parameters:

$p = 1.8$

$q = 1.5$

$A = 1$

Results are shown in Figure 6 and seem to capture the behavior quite well.

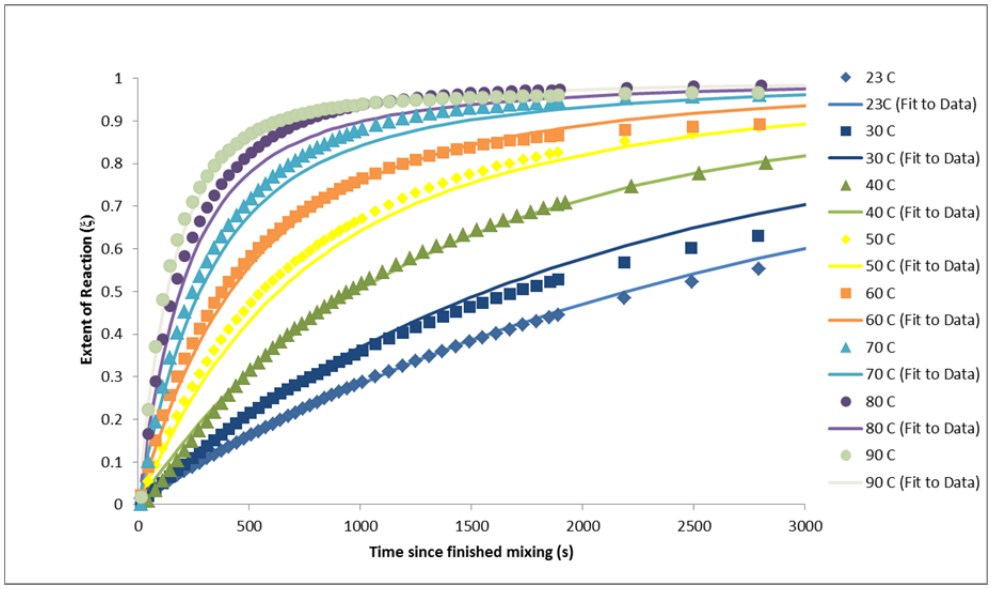

Figure 6. The measured extent of polymerization reaction at early times (during the mold filling operations) compared to the numerical fit from equations 1 and 2 for several temperatures.

However, as mentioned in a previous report [Mondy et al. 2014], the kinetics chosen to best describe the reaction rate behavior during mold filling, necessary to predict the rheology and exotherm, do not predict the longer time behavior that will be needed for structural stability prediction. The later time values for the extent of reaction are compared to the model in Figure 7, and it can be seen that the model predicts much too high conversion rate at late times. We speculate that after the gel point the reaction becomes diffusion dominated and slows. Future work will address how to get better kinetic data that can capture effects of vitrification and how to describe the late time kinetics better.

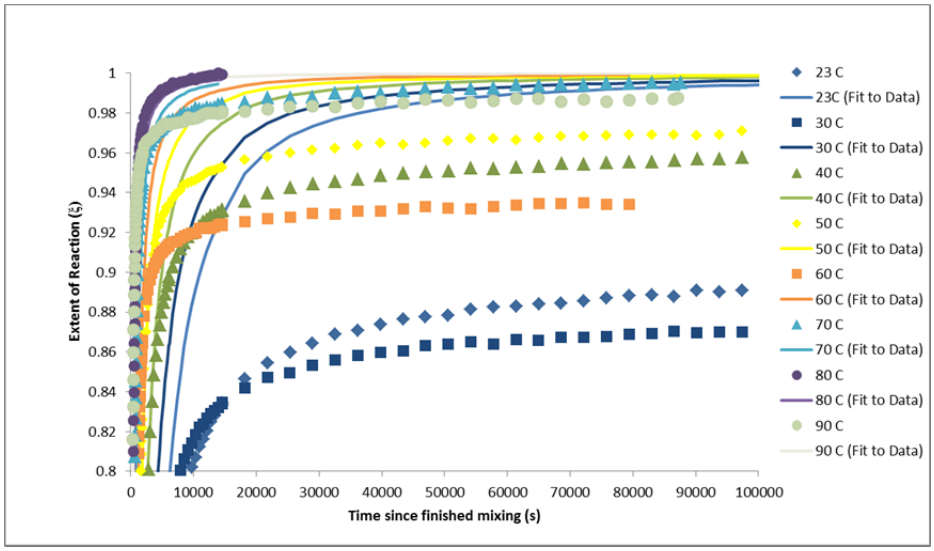

Figure 7. The measured extent of polymerization reaction at later times compared to the numerical fit from equations 1 and 2 for several temperatures.

I.4.2. Gas Generation Reaction

The extent of reaction of the gas producing reaction α, defined as the ratio of the number of moles of gas n_{CO2} to the maximum possible from stoichiometry, seems best described by a Michaelis-Menten reaction form [Levenspiel 1972]:

$$\frac{d\alpha}{dt} = \frac{NK(1-\alpha)^n}{(1-\alpha)^m + M} \tag{3}$$

$$K = A_1 e^{E_1/RT} \tag{4}$$

$$M = A_2 e^{E_2/RT} \tag{5}$$

where N is a time delay to approximate the time it takes for bubbles to nucleate:

$$N = 0.5(1 + \tanh(t - t_{nucleation})) \ . \tag{6}$$

The parameters *N, K, M, n,* and *m* were fit by hand, as this highly nonlinear equation set was difficult to optimize through curve-fitting packages. *K* and *M* were fit at each temperature assuming that *n* and *m* remained the same. Changes were iterated until a reasonable fit was achieved at multiple temperatures. The operating temperature on the production floor is most likely to be a mold temperature of 100 °F (37.8 °C) when the material is foaming [Chace 2014]. The best fit of the data was achieved with the following parameters:

$n = 2.4$

$m = 8$

$A_1 = 130$

$-E_1/R = -3700$

$A_2 = 2.7 \times 10^{-6}$

$-E_2/R = 3700$

$t_{nucleation} = 100$

where –E/R is in units of K, A_1 is in units of s^{-1} and $t_{nucleation}$ is a dimensionless time. The results are shown in Figure 3. Results are better if the nucleation time is allowed to decrease as the temperature increases. Figure 8 shows the results at the extreme temperatures, 40 and 70 °C, with $t_{nucleation}$ of 150 and 70, respectively.

The only major change in the formulation between this PMDI-18 and the lighter weight PMDI-4 used in encapsulation processes, is the amount of water. Assuming that this would not affect the polymerization rate, the same activation energies were used but other parameters varied and then the model was compared to the older PMDI-4 data. Figure 9 shows the results using the parameters:

$n = 2.8$

$m = 10.$

$A_1 = 350.$

$-E_1 / R = -3700.$

$A_2 = 6.0 \times 10^{-6}$

$-E_2 / R = 3700.$

$t_{nucleation} = 60$

This fit is good at the higher temperatures but less so at lower temperatures. Note that the nucleation time is shorter for this foam with higher water content, and the nucleation rate is less sensitive to the temperature. When used for encapsulation processes, the mold temperature during foaming is usually close to 60 or 70 °C.

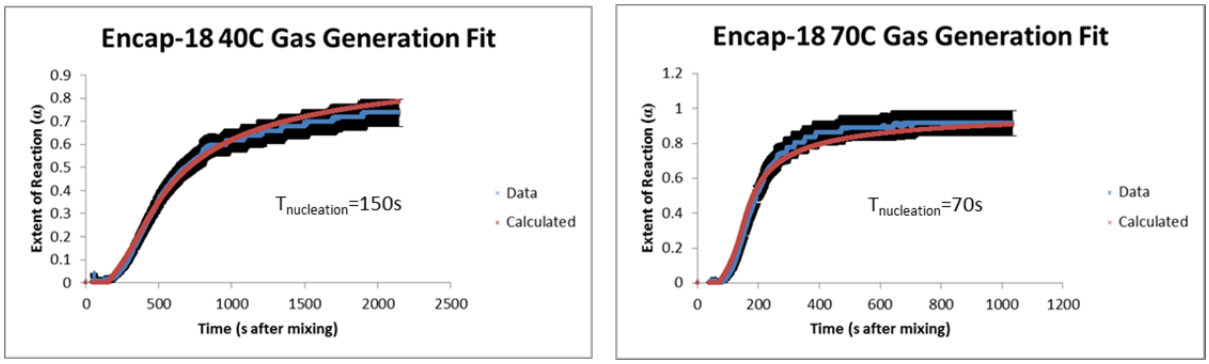

Figure 8. Data compared to model fit at 40 and 70 °C using a nucleation time that depends on the temperature as noted in the annotations.

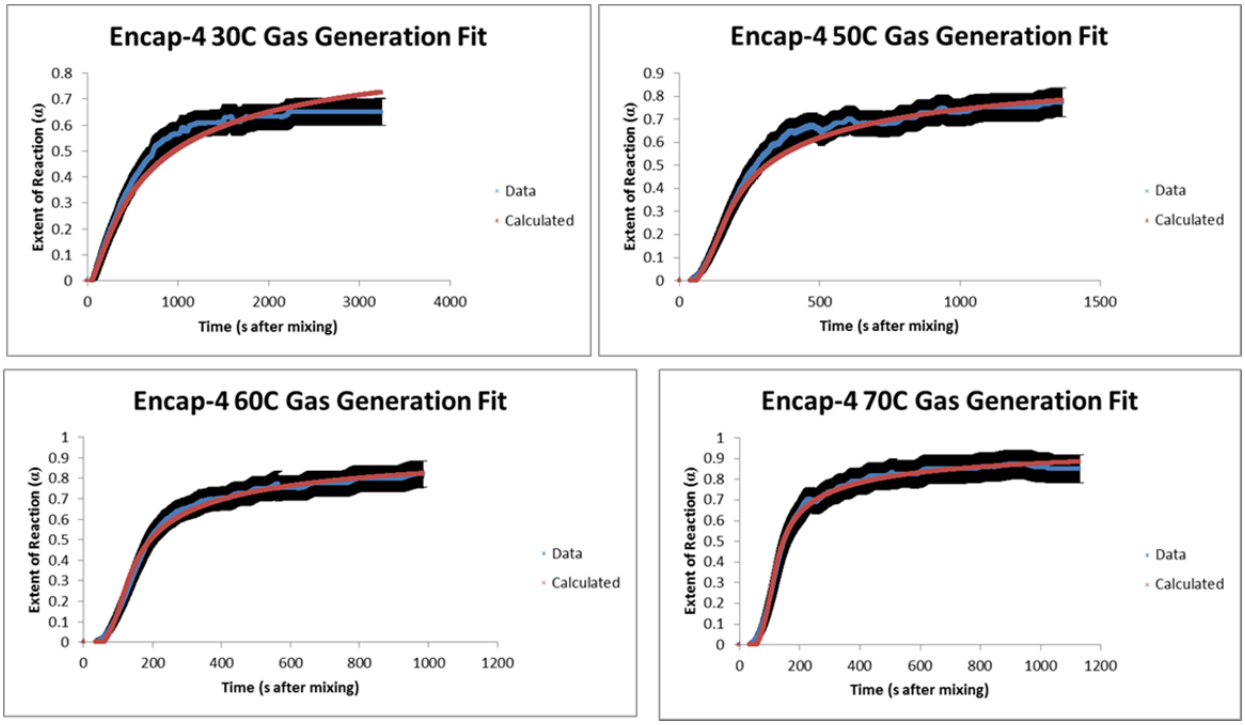

Figure 9. Data (blue line) for BKC 44307 PMDI-4 foam at nominal oven temperatures listed in each title. Black bands indicate 8% uncertainty bars. Red curves are the model results with parameters listed in the text.

I.5. Summary and Conclusions

We have presented data needed to develop and parameterize models with which to predict the polymerization and foaming of polyurethane PMDI-18, a newly developed, reasonably dense, foam based on a previous formulation using the catalyst 33LV.

The polymerization is tracked with IR spectroscopy, and the foam blowing reaction is studied by measuring the volume and pressure increase with time and temperature. The IR data are fit to a condensation chemistry form with four parameters. The data are described well by this model for the first 1000 seconds or so. However, gelation slows the kinetics and the equation predicts continued polymerization at a rate faster than observed. Therefore, for use in models attempting to capture behavior after the foam expansion phase, a more complex reaction rate form is needed and will be the subject of future studies.

Foam-rise experiments used to determine the reaction rate of the gas forming reactions by assuming that all of the increase in volume is from CO_2 production and that the gas obeys the ideal gas law. These results are less definitive than the IR results, since some of the carbon dioxide could be lost to the atmosphere due to bubble breakage at the surface. Also, the temperature is not constant in the experiments to measure foaming volume. In addition, we are only measuring the pressure at the walls and not measuring the true pressure of the gas in the bubbles. The data fit reasonably well to a Michaelas-Menten reaction rate form, although here, too, the reaction rate near the end of the conversion is too fast. In addition, the form with the

parameters suggested here does not predict the reaction rate as well at low temperatures as at the higher ones tested.

PART II. STRUCTURAL RESPONSE EXPERIMENTS

II.1. Coefficient of Thermal Expansion of PMDI-10

Two samples of materials were tested for CTE. The first was a section cut from a KCP-made part, a Support A. Here the foam material was over packed in the mold so that the section's final density at room temperature (about 23 °C) based on its dimensions and mass was 0.9 g/cm^3 (55.5 lb/ft^3). This part is shaped primarily as a pipe with approximately ¼-inch walls (0.63 cm). The second sample was made from a kit where the water had been removed from the resin. This resulted in a final density at 25 °C of 1.02 g/cm^3 (63.8 lb/ft^3). It was taken from a molded right circular cylinder with a diameter of 2.0 in (5.1 cm). The Support A was cured in an oven set to 250 °F (121 °C) for four hours. The dried material was cured at 82 °C overnight (about 18 hours). However, this nonporous foam, with the thicker diameter, could have reached higher temperatures because of the exothermic reactions that influence thinner sections less. It was hoped that the dried material would approximate the material in the continuous phase of the foam, i.e. the "neat" polymer.

Thermomechanical analysis (TMA) was used to measure the change in dimension of the samples both for cooling from 175 °C to -35 °C and then from heating back up from -35 °C to 175 °C. This yields two CTE measurements for each material, as well as two estimated values of T_g. This first test was done with temperature ramp rate of 3 (or -3) °C/min. As can be seen in Figure 10, for the non-porous material, the two CTE values in the linear glassy region (below T_g) are 64.18 and 65.40 ppm/°C, for an average of 64.8 ppm/°C. There is a hysteresis in the CTE in the rubbery region above T_g, giving two values, 221.6 ppm/°C for the first (cooling) ramp and 180.5 ppm/°C for the second (heating) ramp; although, we are less concerned about this hysteresis from the standpoint of stability modeling in normal environments. The estimates for T_g are 143.98 °C for the first ramp down and 148.62 °C for the following ramp up wherein T_g is estimated as the intersection of the approximate slopes in the glassy and rubbery states. The evolution of the rubbery CTE and T_g parameters indicates continued cure.

For the Support A foam (Figure 11), the CTE values in the glassy regime are 63.41 and 64.55 ppm/°C, for an average of 64.0 ppm/°C. These values are very close to the values for the nonporous sample, expected if the CTE is insensitive to the material density. However, the T_g estimates are much lower, close to the cure temperature: 119.5 °C for the ramp down and 127.40 °C for the following ramp up. The differences in these values for T_g were the first hint that the material may be not be fully cured and that increasing the temperature above the T_g may have allowed further curing or a decomposition or oxidation reaction to occur.

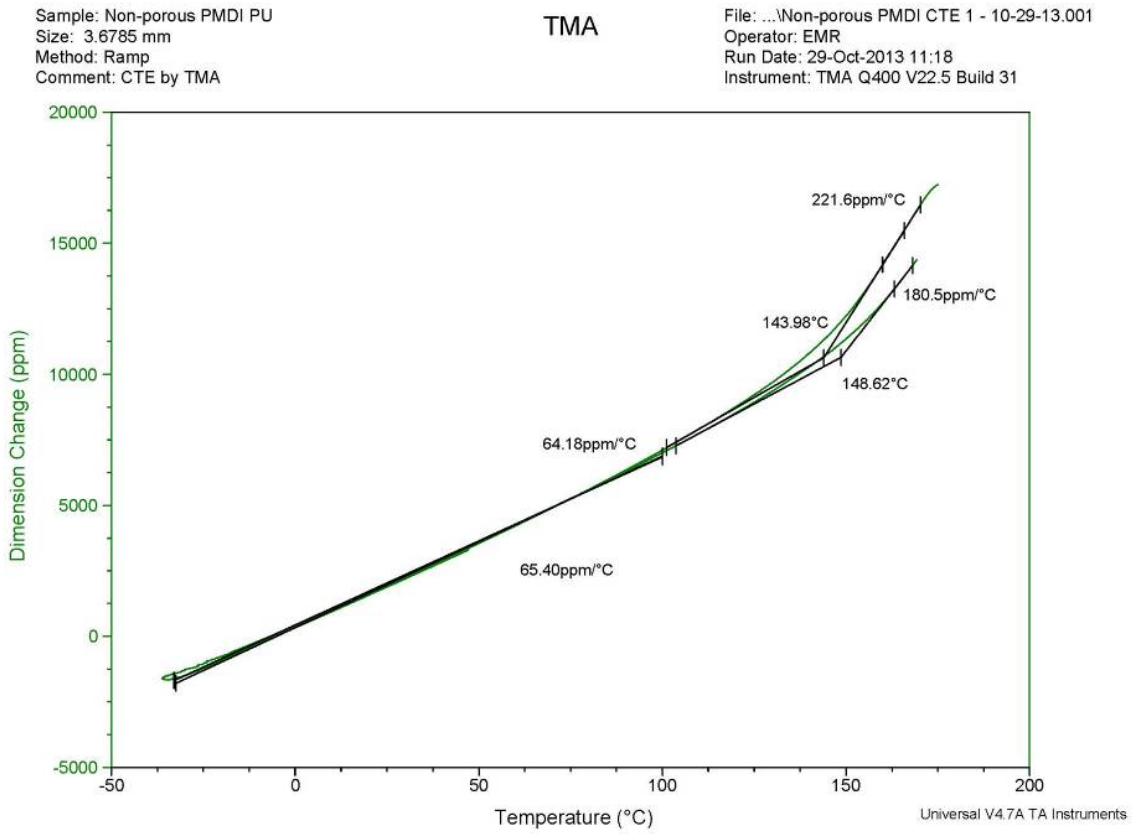

Figure 10. TMA analysis of polymer matrix (from dried PMDI-10 foam kit) at a temperature ramp rate of 3 °C/min down and up.

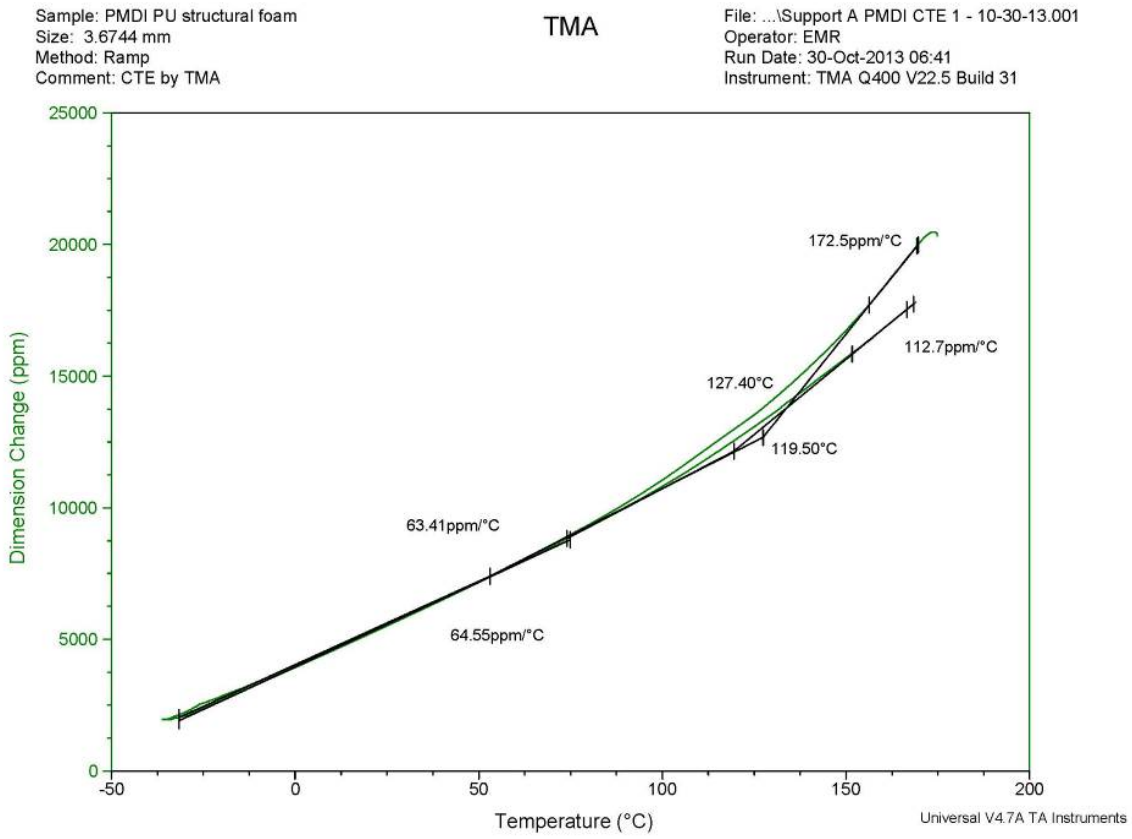

Figure 11. TMA analysis of a Support A part at a temperature ramp rate of 3 °C/min down and up.

Next we looked at the effect of the temperature ramp rate to see if that would diminish the hysteresis. Tests were repeated, first for the same sample of Support A at 1 °C/min. The results are shown in Figure 12. Again the CTE in the glassy regime was close to the same value as before (64.45 and 64.89 ppm/°C); however, the T_g had increased. And the value in the second ramp was higher than the first. Again, this indicated that the values could be increasing because the foam is continuing to cure (or react in some way) with continued heating. The lower ramping rate did not diminish the hysteresis.

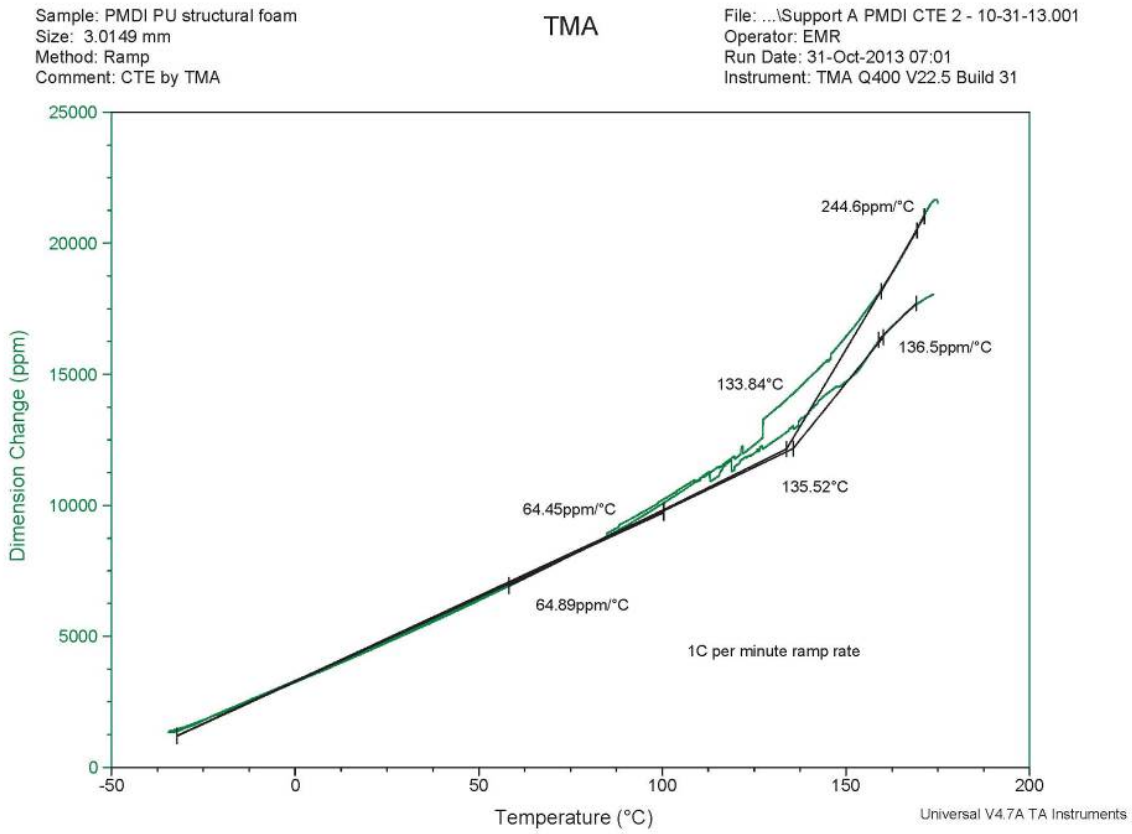

Figure 12. TMA analysis of a Support A part at a temperature ramp rate of 1 °C/min down and up.

Because of the noise seen in Figure 12 , the second test of the nonporous material was performed at 2 °C /min (Figure 13). These results yielded a lower glassy T_g than in the first test of the same material, and caused us to suspect that the differences in Tg among the results could be within the accuracy of the technique. The CTE at the lower temperatures was again very close to the results of the other tests.

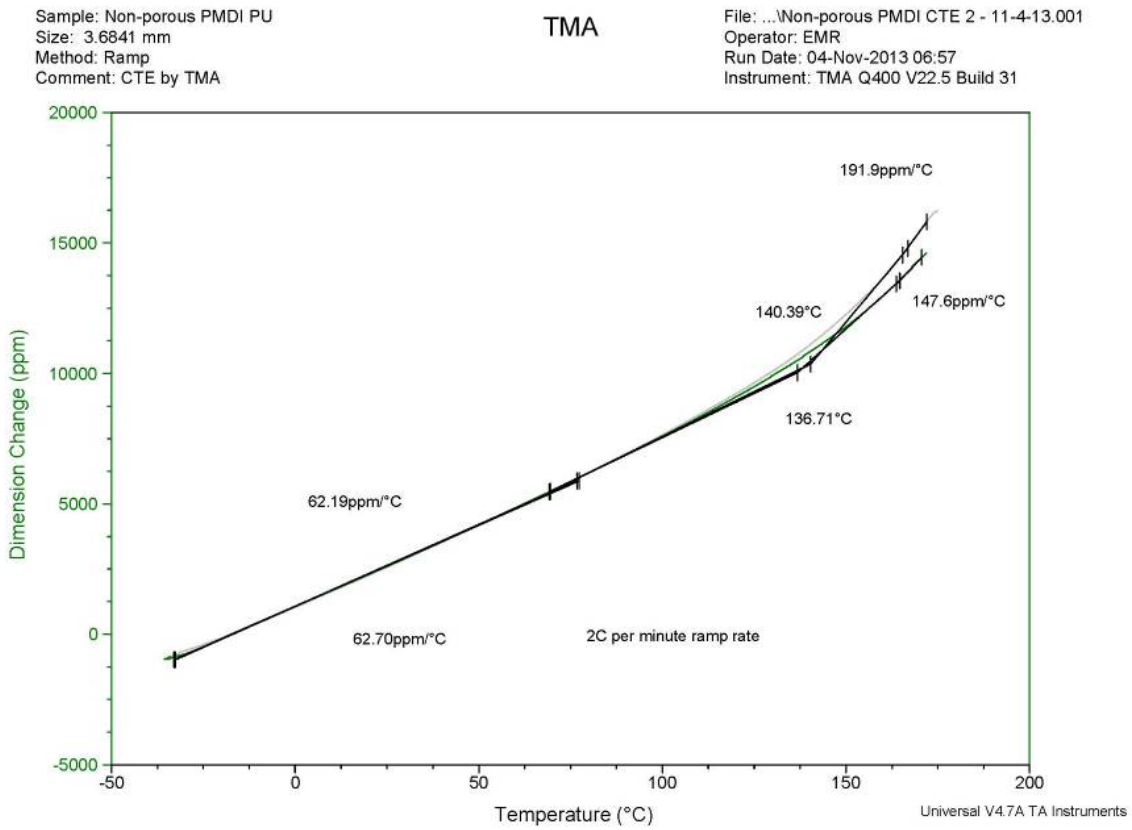

Figure 13. TMA analysis of polymer matrix (from dried PMDI-10 foam kit) at a temperature ramp rate of 2 °C/min down and up.

II.2. Viscoelastic Response of the Cured PMDI-10

II.2.1 Rheology Data

To characterize the linear viscoelastic response of the polymer matrix and get another estimate of T_g, we measured the rheology of the cured BKC 44306 PMDI-10 foam. At the glass transition, the storage modulus (G') decreases dramatically, and the ratio of the storage to loss modulus (G") reaches a maximum. Therefore, temperature-sweeping in a rheometer is often used to characterize T_g of a material. Our objective is to characterize the relaxation behavior of the foam near and above its glass transition (the linear viscoelastic response), which constitutes a first step in characterizing the non-linear viscoelastic behavior that occurs well below the glass transition. To that end, a series of isothermal frequency sweeps were performed near Tg with the goal of building a master curve for the storage and loss moduli and extracting the shear relaxation spectrum from these tests. We note that such an analysis assumes that the time-temperature superposition principal applies, which typically requires that the thermal-mechanical properties are not changing due to further chemistry.

A thin rectangular sample of nonporous (dried) structural PMDI-10 foam, again to approximate the "neat" polymer making up the continuous phase of foamed material, was cured at 121 °C for

14 hours. In the course of the experiment the sample was subjected to temperatures up to 185 °C. The initial temperature is the standard cure temperature (although we held it longer) and the higher temperature was chosen to be above the T_g measured in the previous section with the TMA and above any other reported value we found in the available Sandia records.

Tests were performed with an ARES-G2 rheometer with a torsion fixture in oscillatory mode. Isofrequency (1 Hz) temperature sweeps were made between 75 to 185 °C, either a temperature ramp up or down. After several of these isofrequency temperature ramps, the temperature was held constant while the frequency was varied from 0.001 to 30Hz. During these tests, the set temperature was changed by 2 °C at a time, and the material held there for 5 minutes prior to sweeping through the frequency range. This was repeated at several temperatures from 180 °C to 150 °C in 5 °C increments. Finally, one last isofrequency temperature ramp was performed to determine how significantly the thermal-mechanical properties changed. The experimental matrix and thermal histories were:

1. sample cured at 121 °C for 14 hrs, then isofrequency (strain of 0.2%) temperature sweep 75-185 °C at 2 °C per minute
2. sample held at 180 °C for 6 hrs, then 2nd isofrequency (strain of 0.1%) temperature sweep 185-75 °C at 2 °C per minute
3. 3rd isofrequency (strain of 0.1%) temperature sweep 75-185 °C at 2 °C per minute
4. 4th isofrequency (strain of 0.1%) temperature sweep 185-75 °C at 2 °C per minute
5. isothermal frequency sweeps (0.001 to 30 Hz) from 180 to 150 °C (every 5 °C)
6. final isofrequency (strain of 0.1%) temperature sweep 100-185 °C at 2 °C per minute

Resulting data are shown in Figure 14 and Figure 15. In the latter figure, one can see that the glass transition temperature continues to increase over the duration of the experiment reaching a maximum of about 176 °C, as illustrated by the maximum of the ratio of the loss to the storage modulus, or tan δ.

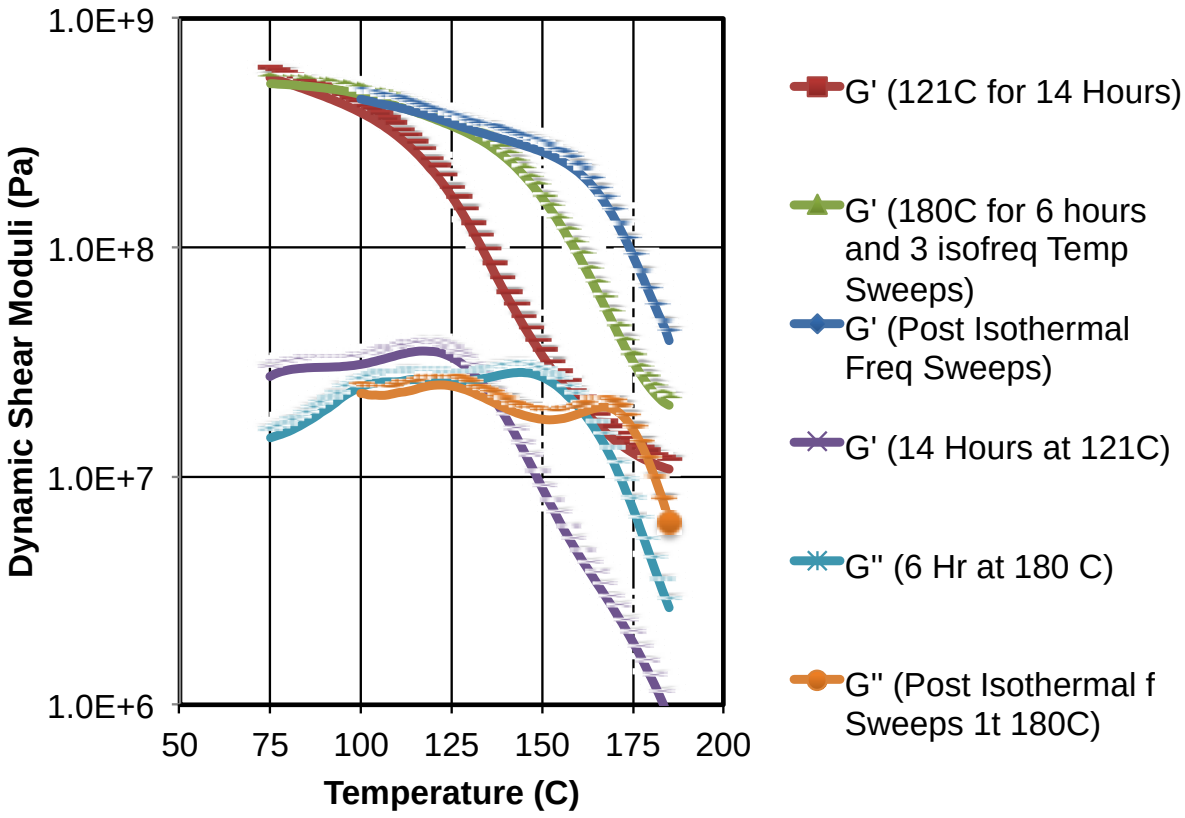

Figure 14. Dynamic shear storage (G') and shear loss (G") moduli measured in oscillatory tests of cured nonporous foam.

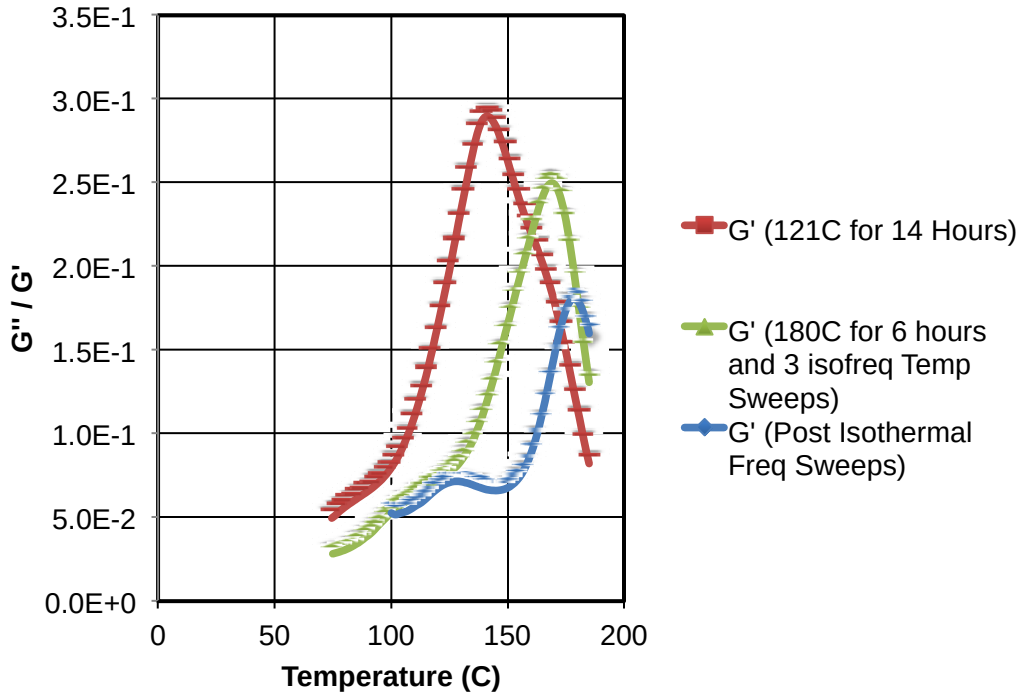

Figure 15. Tan δ or the ratio G"/G' vs. temperature. Tan δ reaches a maximum at T_g.

Tan δ is a non-obvious function of frequency compared with traditional thermoset behavior near the glass transition as can be seen in Figure 16.

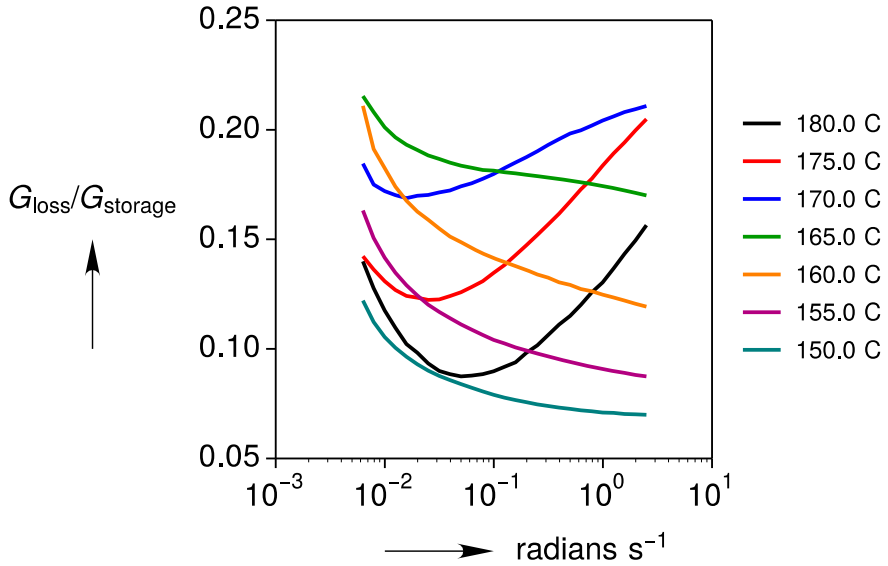

Figure 16. Ratio of G"/G' at various frequencies and temperatures.

II.2.2. Analysis

The data detailed above were used in an initial attempt to fit a model of the viscoelastic response of epoxies described by Adolf and Chambers [2007] and Kropka et al. [2013]. Here one must assume that the relaxation behavior of the network does not substantially change with the cure that apparently continues to take place at higher temperatures. In addition, we assume that the Time Temperature Superposition Principal (TTS) applies, and we attempt to horizontally shift each isothermal storage modulus frequency-sweep data to produce a master curve. Normally, vertical shifting due to temperature dependence of the moduli would be required, but we found that no vertical shifting was necessary to form an approximate master curve in Figure 17. Ideally, one would shift the tan δ since no vertical shifting is needed if the storage and loss moduli have the same temperature scaling, but in this work, the tan δ curves involved non-traditional behavior that did not admit reasonable horizontal shifting (Figure 17). After the master curve for the storage modulus was formed, the shift factors vs. temperature were fit to a Williams-Landel-Ferry (WLF) function, which is reasonably fit with the parameters. Finally, the storage modulus master curve was inverted to produce a collection of proney weights to describe the relaxation behavior observed experimentally (Figure 18).

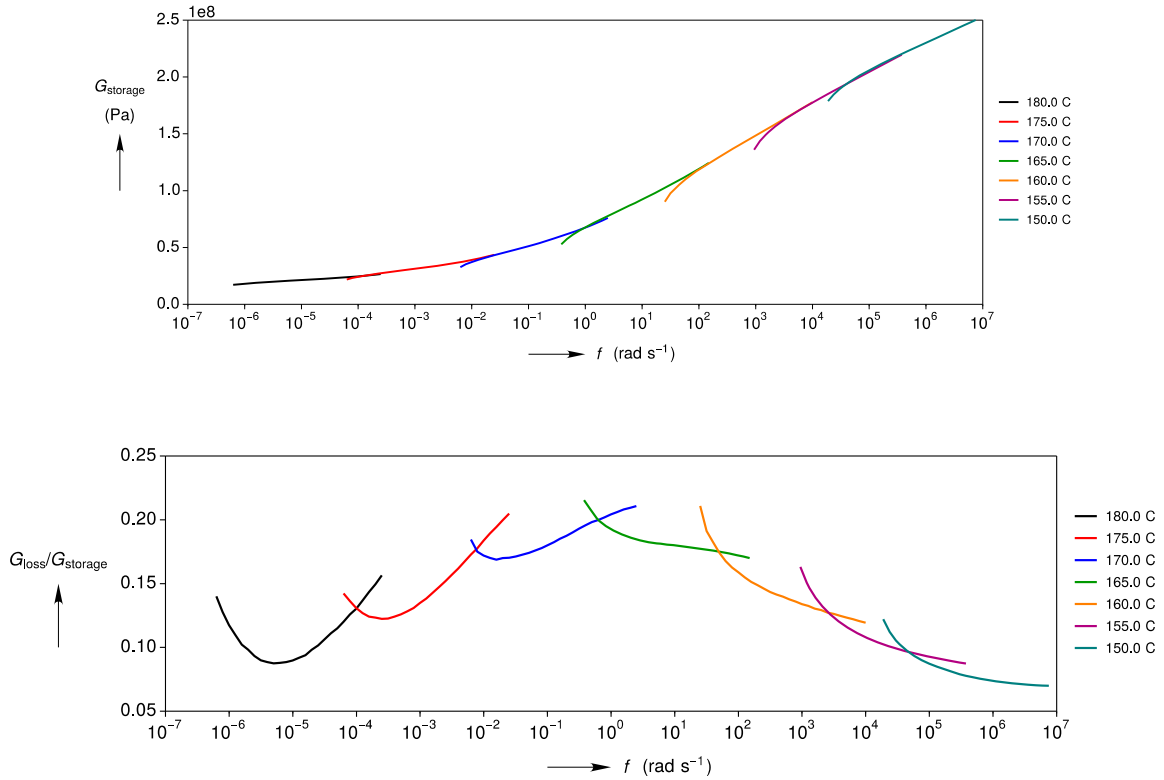

Figure 17. Shifted storage modulus (above) and the associated tan δ (below) master curves. The latter does not produce a typical master curve.

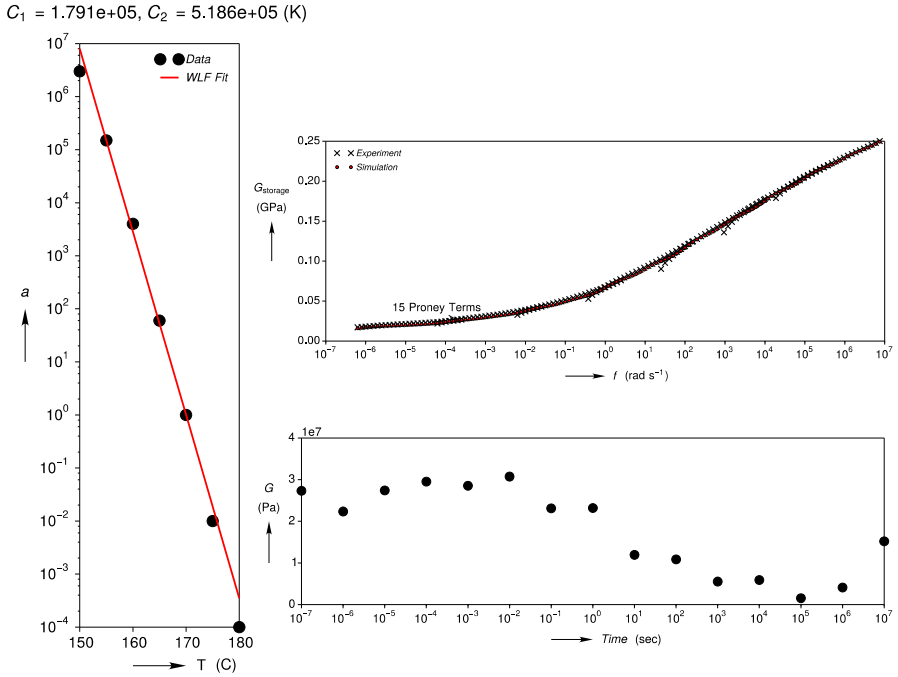

Figure 18. Fit of the WLF equation to the shift factors that formed the storage modulus master curve (left). After inverting the frequency response from the master curve, the shear relaxation function is recovered in the time domain. A proney series is used to represent this relaxation response (top right) with proney weights at each time scale shown in the bottom right.

Compared with Ferry [1980], the WLF coefficients C1 and C2 are substantially different for polyurethane thermosets and here produce a narrower glass transition. The use of this characterization should be considered with caution! A different approach is needed to bypass the complexities of continued cure in subsequent fiscal years.

II.2.3. Chemical Changes

We are now convinced that we have not characterized a fully crosslinked polymer, which is necessary to use the analysis tried above. Attempts to bring the material to even higher temperatures resulted in significant off-gassing and decomposition without improvement in the data. Figure 19 shows a torsion bar sample tested under a N_2 atmosphere in an attempt to eliminate possible oxidation of the sample. Color change first observed in air occurs under N_2 as well.

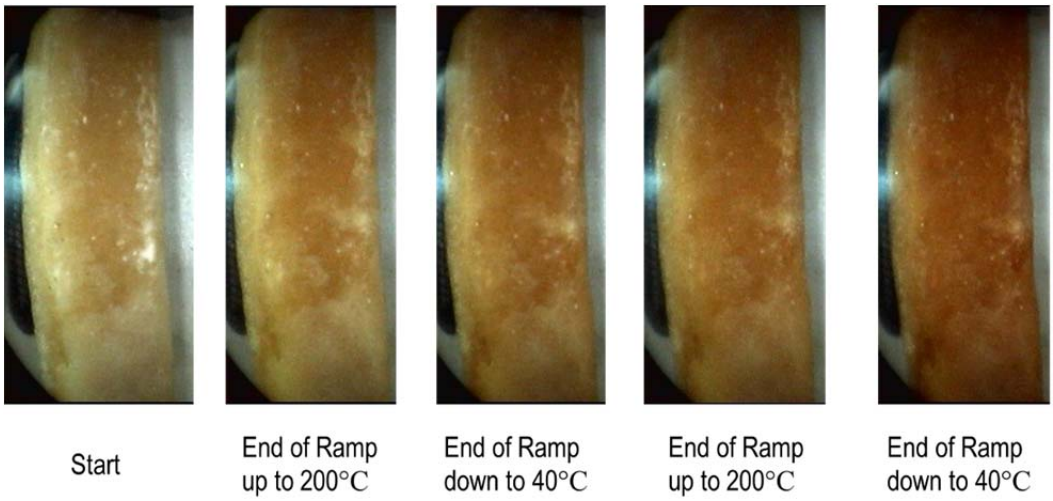

Figure 19. Images of a foam sample after rheology testing in an N_2 environment.

We used IR spectroscopy to measure the levels of residual isocyanate on samples of structural PMDI-10 foams after various times at several cure temperatures (Figure 20). A fully cured sample would have no residual isocyanate. This occurred only after excessive time at a higher-than-normal curing temperature. The samples also became discolored before this time.

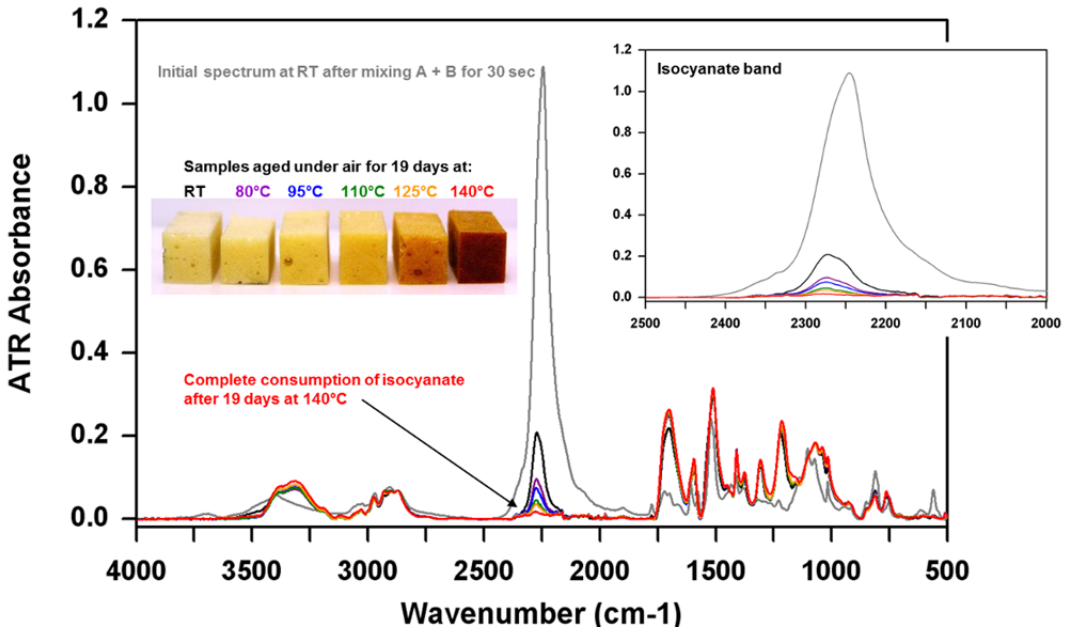

Figure 20. IR Spectroscopy shows that the isocyanate is not consumed in curing PMDI-10 foam until it has been held for 19 days at an elevated temperature of 140 °C. However, this extended cure time leads to foam color change indicative of some type of accelerated aging.

II.3. Summary and Conclusions

We describe experiments of discovery and the first attempt to determine parameters for a preliminary model to predict dimensional stability during manufacturing and aging. Both CTE and viscoelastic response of the polymer matrix (as approximated by using foam with the foaming agent, water, removed) were measured. Unfortunately, the proposed model is based on knowing the properties of the fully cured material. Repeated TMA tests to measure CTE produced a fairly constant value of the glassy CTE, but could not characterize a consistent T_g. Oscillatory testing of a torsion bar in an ARES-G2 rheometer showed a T_g that continued to increase with the length of time held at elevated temperatures. The standard cure schedule used at KCP (121 °C for four hours) clearly did not produce a fully cured material. Attempts to fit rheology from a "cured enough" sample yielded unrealistic fitting parameters. Further investigation using IR spectroscopy showed that the residual isocyanate did not fully react until the material had been held at 140 °C for 19 days. By that time the material had discolored, making it suspect for use in viscoelastic characterization. Clearly, further work is needed, as well as a new approach to obtain parameters for a model of the viscoelastic response of the foam when it is removed from a mold, cooled, and aged. This will be the focus of future work.

REFERENCES

Adolf, D. B. 1996, *Measurement Techniques for Evaluating Encapsulant Thermophysical Properties During Cure*, Sandia National Laboratories, SAND96-1458.

Adolf D.B. and Chambers R.S. 2007, "A thermodynamically consistent, nonlinear viscoelastic approach for modeling thermosets during cure*"*, *J. Rheology*, **51**, 23-50.

Adolf, D. B. and Chambers, R. S. and Neidigk, M. A. 2009, "A simplified potential energy clock model for glassy polymers," *Polymer*, **50**, 4257-4269.

Chace, A. 2014. email to L. Mondy, September 9.

Ferry, J.D. *Viscoelastic Properties of Polymers*, 3rd Edition, John Wiley and Sons. 1980, Pages 278-279

Kropka, J. M., Spangler, S. W., Stavig, M. E., Chambers, R. S. 2013. Residual Stress: Prediction during Polymer Cure and Effects on the Strength of Adhesive Joints, Sandia National Laboratories, SAND2013-8681.

Levenspiel, O. *Chemical Reaction Engineering*, 2nd Edition, John Wiley and Sons. 1972, Pages 16, 65.

Long et al., 2014, "Modeling the Dimensional Stability of Chemically Blown Foam," 30th International Conference of the Polymer Processing Society, Cleveland, OH, 06/08-12/2014.

May, C. A., Ed., *Epoxy Resins Chemistry and Technology*, 2nd Edition, Marcel Dekker: New York, 1988.

Mondy, L. A.; R. R. Rao; B. Shelden; M. Soehnel; T. J. O'Hern; A. Grillet; M. Celina; N. Wyatt; E. Russick; S. Bauer; M. Hileman; A. Urquhart; K. Thompson; D. Smith. 2014, *Experiments to Populate and Validate a Processing Model for Polyurethane Foam: BKC 44306 PMDI-10*, Sandia National Laboratories, SAND2014-3292.

Mondy, L. A.; M. Celina; J. Kropka; R. R. Rao; E. Russick; N. Giron; R. Cote; J. Castaneda; J. Aubert. 2010, *Novel Foam Encapsulation Materials and Processes*, Sandia National Laboratories, SAND2010-6868.

Pockett K. and Warriner C., 2013 *Understanding the dimensional stability of rigid polyurethane foam*, AWE Report 283/13.

Rao, R. R.; L. A. Mondy; M. C. Celina; D. B. Adolf; J. M. Kropka; E. M. Russick. 2010. Proceedings of the Polymer Processing Society 26th Annual Meeting, PPS-26 Proceedings, Banff.

Rao, R. R.; L. A. Mondy; M. C. Celina; D. R. Noble, S. A. Roberts, K. Thompson, J. Tinsley. 2013. Proceedings of the Polymer Processing Society 29th Annual Meeting, PPS-29 Proceedings, Nuremberg.

Tesser, R.; M. Di Serio; A. Sclafani; E. Santacesaria. 2004. *J. Appl. Polymer Sci.*, **92**, 1875.

DISTRIBUTION (ELECTRONIC COPIES)

1	MS0161	Legal Technology Transfer Center	11500
1	MS0346	Lisa Mondy	1512
1	MS0346	Christine Roberts	1512
1	MS0346	Anne Grillet	1512
1	MS0346	Melissa Soehnel	1512
1	MS0346	Tracie Durbin	1512
1	MS0382	Shayna Begay	2153
1	MS0382	Heather Boldt	2153
1	MS0386	Joe Fonseca	2128
1	MS0555	Kyle Thompson	1522
1	MS0807	David Michael Smith	9328
1	MS0836	Timothy O'Hern	1512
1	MS0836	Bion Shelden	1512
1	MS0836	Rekha Rao	1514
1	MS0836	Daniel Rader	1514
1	MS0888	Edward Russick	1833
1	MS0888	James McElhanon	1835
1	MS9042	Amanda Dodd	8365
1	MS9403	LeRoy Whinnery	8223
1	MS0958	Nicholas Wyatt	1835
1	MS1033	Stephen Bauer	6914
1	MS1033	Michael Hileman	6914

1	MS1033	M. Lee	6914
1	MS1411	Mat Celina	1819
1	MS0899	Technical Library	9536

External:
James Tinsley, NNSA's Kansas City Plant Operated by Honeywell Federal Manufacturing & Technologies, LLC, D/891 Advanced Engineering Simulations & Analysis, Kansas City, Mo.


Sandia National Laboratories